One-step synthesis of spin crossover nanoparticles using flow chemistry and supercritical CO2

Nathalie Daro, Tony Vaudel, Luc Afindouli, Samuel Marre, Cyril Aymonier, Guillaume Chastanet

COMMUNICATION

One-Step Synthesis of Spin Crossover Nanoparticles Using Flow Chemistry and Supercritical CO_2

Nathalie Daro,[a] Tony Vaudel,[a] Luc Afindouli,[a] Samuel Marre,[a] Cyril Aymonier,*[a] and Guillaume Chastanet*[a]

[a] Dr. N. Daro, T. Vaudel, L. Afindouli, Dr. S. Marre, Dr. C. Aymonier, Dr. G. Chastanet
CNRS – Université de Bordeaux – Bordeaux INP, ICMCB UMR 5026,
87 av. Dr. A. Schweitzer, F-33600, Pessac, France
E-mail: cyril.aymonier@icmcb.cnrs.fr; guillaume.chastanet@icmcb.cnrs.fr

Supporting information for this article is given via a link at the end of the document.

Abstract: Switchable materials are increasingly considered for implementation in devices or multifunctional composites leading to a strong need in terms of reliable synthetic productions of well-defined objects. We report here an innovative and robust template-free continuous process to synthesize nanoparticles of a switchable coordination polymer, including the use of supercritical CO_2, aiming at both quenching the particle growth and drying the powder. This all-in-one process offered a 12-fold size reduction in few minutes, maintaining the switching properties of the selected spin crossover coordination polymer.

Molecular switches are increasingly implemented in functional materials for sensing applications[1] or in molecular electronics[2]. Among the switchable systems under study, spin crossover (SCO) materials are widely investigated in regard to their ability to change their electronic configuration in response to external stimuli (temperature, pressure, magnetic field, light, adsorption of molecules)[3-5]. The vast majority of SCO compounds reported so far concerns Fe(II) and Fe(III) complexes and especially the 1D coordination polymers based on 4-R-1,2,4-triazole ligands and iron(II) salts (SCO-triazole family). Indeed they exhibit a room temperature (or close to) thermochromism[6-8], related to the switching between high-spin (HS, paramagnetic) and low-spin (LS, diamagnetic) states, which can result in memory effects of interest in displays[9] and sensors[1].

Over the years, such systems have become more and more relevant to applications[1,2,10]. Such increasing interest is faced with the need for an upscaled and reliable production of particles with well-defined and tunable size, morphology and properties. Currently, two main synthetic routes are followed to obtain these particles[11]: (*i*) direct fabrication based on batch mode synthesis, leading to a poor control of size, morphology and size distribution; (*ii*) a templating approach based on soft or hard organic or inorganic templates, offering excellent control of the nanoparticle characteristics. The templating approach is widely used for the synthesis of SCO nanoparticles, but is mitigated by two main issues. The first is that reproducibility is not always fully achieved, especially at a very small scale (below 100 nm) [12]. The second issue concerns the template removal, which can be difficult or impossible in the case of hard templates (such as porous silica or polymers) or charged surfactants. Therefore, the synthesis of such materials in large quantities, with a high reproducibility, and using template-free methods able to tune the size and size-distribution of the particles, is still a challenging aim. To achieve this goal, direct precipitation is the most trivial method, but does not provide good control over the size and morphology[13]. The authors have explored other techniques, such as spray drying[14] or microfluidics[15]. While spray drying offered interesting morphologies and phases, it appeared difficult to control in the case of the SCO-triazole family. Regarding the microfluidic approach, a drastic downsizing effect was observed using droplet microfluidics in which each droplet of water containing the reactants is carried by a flow of oil. Even if, strictly speaking, no surfactants are used in this method, the oil must still be removed afterwards. We have therefore turned our attention to the use of flow chemistry allowing a fine control of process parameters, which is an alternative and original route to the aforementioned approaches.

Flow chemistry has already been successfully applied to different kinds of materials[16,17] such as luminescent quantum dots[18-22], metal nanoparticles[23,24], polymers[25,26], metal-organic frameworks[27,28], organometallic species[29] and molecules[30-33]. Several advantages of moving from batch to flow mode have been recognized, such as facile automation and feedback optimization, increased reproducibility, and improved safety and process reliability. Indeed, with continuous flow processes, stable reaction parameters (temperature, time, amount of reagents and solvents, efficient mixing, etc.) can be ensured[33]. Moreover, these approaches are easily scalable to reach the quantities needed for development and optimization. However, most of the conventional flow processes are still limited to normal conditions of pressure and temperature, thus limiting the process parameter space and the considered solvent systems. On the other hand, high pressure systems can easily handle high flowrates, providing both intense mixing[34], favorable for homogenous nucleation, and particle size control down to the nanometer range[35], along with higher production rates.

Continuous flow synthesis of SCO nanoparticles (NPs) has been recently demonstrated using a milli-scale segmented flow crystallizer reactor[36]. The reported synthesis was based on a liquid-liquid droplet strategy, therefore requiring similar post-treatment as for the conventional batch mode synthesis. However, it does not provide a way to size reduction - mostly in the micrometer range - nor does it allow access to a fast, continuous synthesis process for further scale up, as the reported synthesis time (~ 20 min) was not improved. Therefore, being able to develop an all-in-one multi-step process for synthesizing SCO NPs could provide a way for realizing the promises of these materials in a fast, reliable and robust way.

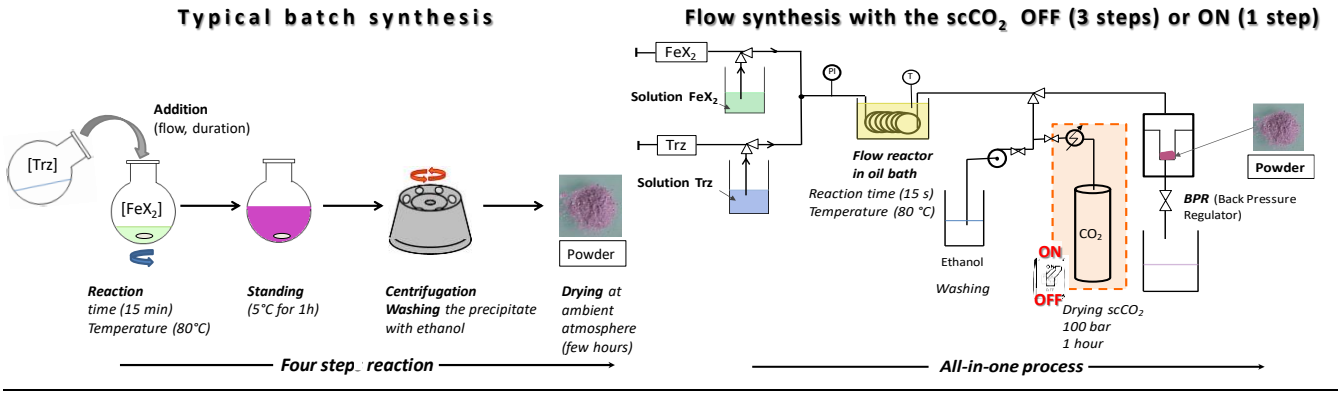

Figure 1: Schematic descriptions and comparison of the conventional batch synthesis process (left) and the continuous $scCO_2$-assisted flow synthesis (right).

We here demonstrate a template-free continuous process to synthesize SCO NPs, including the use of supercritical CO_2 ($scCO_2$). We can reach improvements both in the synthesis efficiency and in access to nanosized SCO particles (by a factor of at least 10 compared to the literature), thanks to the role of $scCO_2$. It permits not only the quenching of the particle growth during the precipitation, but also the recovery of dry powder with no need for additional post treatment. For this purpose, we choose a model compound, $[Fe(Htrz)_2(trz)](BF_4)$[37,38], which has been largely investigated using conventional methods. It is a polymeric compound, known to be the most stable of the triazole family; it does not contain solvent molecules and shows reproducible SCO hysteresis features, even upon size reduction[12,39]. The characteristics of the materials (size, phase, magnetic properties) obtained with the reference conventional batch synthesis are compared with those obtained through this new all-in-one continuous synthesis approach, coupling a flow reactor for precipitation with a supercritical CO_2 drying step.

The polymeric $[Fe(Htrz)_2(trz)](BF_4)$ material was prepared using three different methods (Table 1), while keeping the reactant concentrations constant ($Fe(BF_4)_2.6H_2O$ (10 mmol) and Htrz (33 mmol), with both dissolved in 10 mL water, see SI for details):

(1) A batch method, consisting of four different steps (Figure 1 – top): (*i*) dropwise addition (at 1 mL/min) *via* a syringe pump of an aqueous solution of 1,2,4-1*H*-triazole to an aqueous solution of $Fe(BF_4)_2.6H_2O$ containing ascorbic acid at 80 °C. The resulting solution was stirred for 15 min. (*ii*) aging of the solution for 1h at low temperature (5 °C). (*iii*) centrifugation of the suspension followed by three washing + centrifugation steps with ethanol (EtOH). (*iv*) sample drying overnight at ambient atmosphere[30]. This method led to sample **1** (Figure 2, top) displaying micrometric size rod-shaped particles, whose mean length and width of 2116 ± 382 nm and 487 ± 232 nm, respectively (Figures 3 and SI1).

(2) A continuous reaction process including a washing step with EtOH (Figure 1, bottom, with the switch "off"). The reactor consisted of a 1/16" stainless steel coiled tubing (internal diameter = 1 mm, length = 1.1 m) immersed in an oil bath used to control the temperature. This flow reactor is fed with the two reactant solutions – delivered at constant flowrate (1mL/min) – by conventional syringe pumps (KDS100, KD Scientific) which then mix in a Tee mixer, with a residence time in the reaction zone of 15 s. Downstream of the reaction zone, EtOH was introduced with an HPLC pump, to prepare the further washing step. The particles were collected in a beaker at the outlet of the process. The particles in suspension were stirred for 1 min at 80 °C before undergoing a double washing + centrifugation step with EtOH, and were later let to dry overnight at ambient atmosphere, similarly to sample **1**. The obtained particles (sample **2**) exhibit a rod-shaped submicrometric morphology (Figure 2, middle) with a mean length and width of 277 ± 32 nm and 116 ± 25 nm, respectively (Figures 3 and SI1).

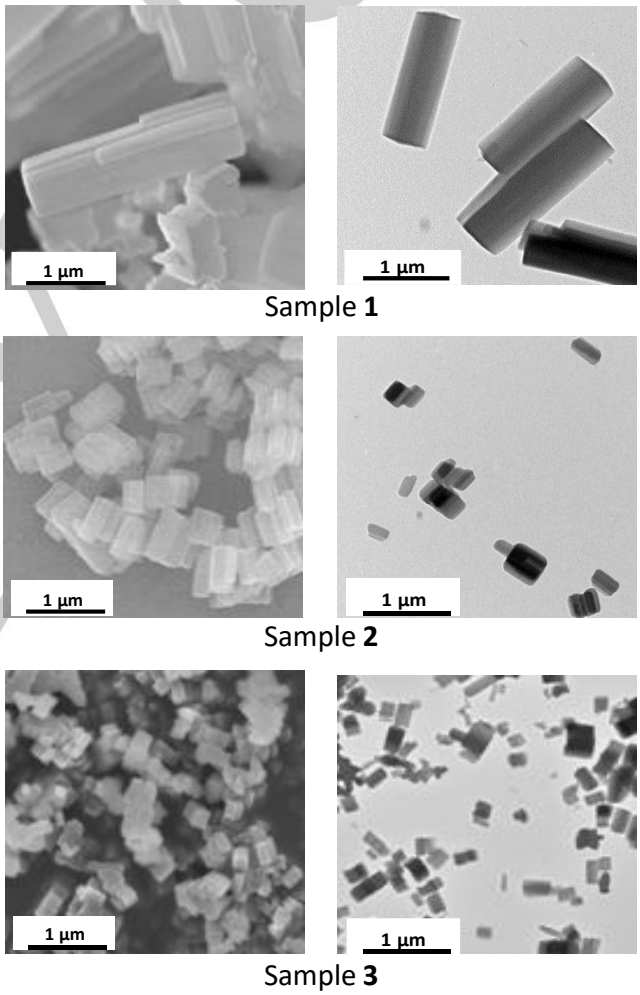

Figure 2: SEM (left) and TEM (right) images of the samples obtained from batch mode (**1**), continuous reaction process (**2**) and the all-in-one process (**3**).

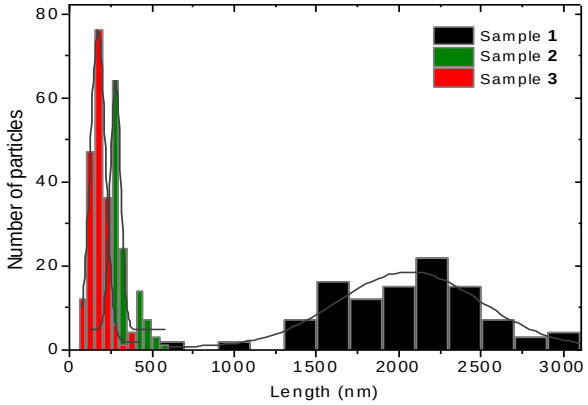

Figure 3: Histograms of the lengths of samples **1-3** and their corresponding statistical distributions obtained by TEM, on at least 100 particles (using the standard deviation from the Gaussian distribution fit).

(3) An all-in-one process including a drying step with supercritical CO_2 (Figure 1, bottom, with the switch "on"). This approach was performed under pressure (p = 100 bar) in order to implement the $scCO_2$ drying step at the very end of the process. The overall principle can be detailed as follows (Fig. 1 – bottom with the supercritical box switched on): first, two high pressure syringe pumps (PhD 2000, Harvard apparatus) were used to separately deliver the two reagent solutions, which mixed in a Tee before entering the reactor (similar to the second approach). Then, EtOH was continuously injected with an HPLC pump as explained in (*ii*). The particles were captured within a high pressure collection vessel equipped with a filter. An automated back pressure regulator (BP2080, Jasco) was placed downstream of the vessel to control the pressure over the entire process. The EtOH flow was used to keep the process conditions similar to the first two approaches and also to make the $scCO_2$-based drying efficient. The $scCO_2$ was eventually injected through the vessel thanks to a continuous high pressure membrane pump (Dosapro, Milton Roy) for 1 hour under a constant CO_2 flowrate (12 mL/min). In the considered conditions (p = 100 bar, T = 80°C), the EtOH / CO_2 mixture was fully homogeneous. The obtained pink-violet powder was recovered in the filter upon depressurization of the system. The particles of sample **3** presented well-defined nanorod shapes (Figure 2, bottom), with mean length and width of 169 ± 45 nm and 48 ± 16 nm, respectively (Figures 3 and SI1).

All the characteristic sizes of the obtained rods are summarized in Table 1 along with the reaction yields. The latter are very similar for all the processes, around 30%. This validates the possibility to significantly reduce the reaction time by switching from batch to continuous modes.

When working with the $[Fe(Htrz)_2(trz)](BF_4)$ compound, one must check the purity and the phase obtained[37]. The chemical analysis demonstrated a good agreement with the expected compound (see SI). The X-Ray diffraction patterns (Figure 4) showed that, whatever the synthesis protocol, the crystalline phase of the obtained powders are the same. From these patterns, an enlargement of the Bragg peaks can be noticed for samples **2** and **3** compared to sample **1**. This is in accordance with the particle size reduction observed in Figures 2 and 3, and previously reported observations[39-42].

Regarding the switching properties, we have recorded the molar magnetic susceptibility (χ_M) as a function of the temperature

Table 1: Comparison of the experimental features and particle sizes of the different synthetic processes (batch synthesis, flow chemistry and flow chemistry with $scCO_2$) for the same switchable material with the same concentration of reactants and reaction temperature

	Batch synthesis	Continuous process	All-in-one process
Reaction yield	30 %	23 %	34 %
production (g)	1.1	0.8	1.2
Steps	4	3	1
Reaction (residence) time	1h15	15 s	15 s
Rod size (length x width)	~ 2 100 nm x 490 nm	~ 280 nm x 120 nm	~ 170 nm x 50 nm

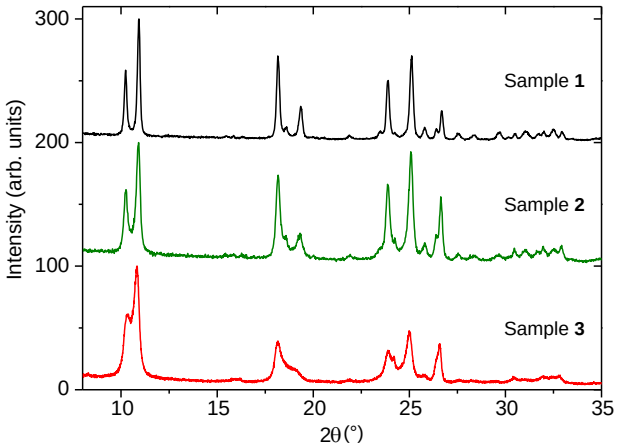

Figure 4: X-ray diffraction patterns for samples **1-3.**

for samples **1**, **2** and **3** (Figure 5). Sample **1** presents the expected SCO behaviour[37]: $T_{1/2up}$ = 386 K and $T_{1/2down}$ = 353 K, describing a large hysteresis loop of 43 K. Sample **2** presents the same features between 349 K and 377 K, with a hysteresis loop of 28 K. Sample **3** exhibits a transition at $T_{1/2\ up}$ = 369 K and $T_{1/2down}$ = 346 K and a hysteresis loop width of 23 K. The differences in the SCO behaviours (transition temperature and hysteresis width) has to be linked to the size of the particles. Indeed, this trend has already been described for rods of the same compound obtained with reverse-micellar synthesis[42].

The use of the continuous reaction process combined with a supercritical CO_2 treatment clearly allows a significant downscaling (more than 10 times in both dimensions of the rods) of the particle size compared to the batch synthesis. This process also affords well-defined particles in a reproducible and reliable way with the same yield as the batch synthesis.

The first main difference between the batch and the continuous modes concerns the hydrodynamics, especially the mixing conditions. This mixing in batch mode is much weaker than in continuous flow[43]. The direct consequence is a lower nucleation rate in batch mode compared to the continuous one, which could be an explanation for the size reduction between samples **1** and **2**. Another important step in the preparation of SCO materials is the aging step. During this step, the formed particles are still in contact with unreacted precursors, promoting further growth of the particles. Beyond the continuous reaction process, an additional advantage of the all-in-one process is the removal of the aging step. Indeed, the addition of $scCO_2$ not only permits the

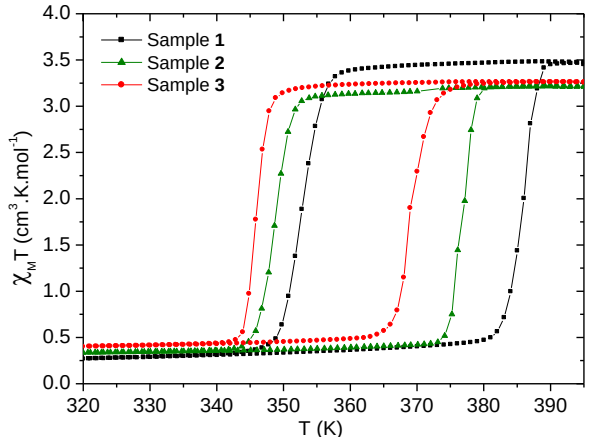

Figure 5: $\chi_M T$ versus T plot for samples **1** to **3**, recorded after a first heating at 395 K.

drying of the sample but also avoids the additional growth of the rods, opening the door to nano-sized materials, as evidenced by the difference in size between compounds **2** and **3**.

The demonstrated all-in-one template-free process provides a robust way for synthesizing switchable SCO nanoparticles with a significant reduction of preparation time. The introduction of a supercritical drying step affords a one-step process for the production of dried and well-defined nanoparticles at large scale. This unique process opens routes towards process intensification and offers new opportunities for molecular materials.

Acknowledgements

This work was supported by the University of Bordeaux, the CNRS, the ANR FlowSwitch (2019-CE07-0022-01), and by the Region Nouvelle Aquitaine and the ADEME agency through the ISOCEL project. The UMS PLACAMAT is acknowledged for the microprobe measurements. Marion Gayot and Sonia Buffière are acknowledged for the help for TEM and SEM images.

Keywords: spin crossover • nanoparticles • flow chemistry • supercritical CO_2 •

[1] J. Linares, E. Codjovi, Y. Garcia, *Sensors* **2012**, *12*, 4479-4492; (b) D. Gentili, N. Demitri, B. Schäfer, F. Liscio, I. Bergenti, G. Ruani, M. Ruben, M. Cavallini, *J. Mater. Chem. C* **2015**, *3*, 7836–7844; (c) M. D. Manrique-Juárez, S. Rat, L. Salmon, G. Molnár, C. M. Quintero, L. Nicu, H. J. Shepherd, A. Bousseksou, *Coord. Chem. Rev*. **2016**, *308*, 395–408; (d) A. Lapresta-Fernández, M. Pegalajar Cuéllar, J. M. Herrera, A. Salinas-Castillo, M. del Carmen Pegalajar, S. Titos-Padilla, E. Colacio, L. F. Capitán-Vallvey, *J. Mater. Chem. C* **2014**, *2*, 7292-7303.

[2] G. Molnár, S. Rat, L. Salmon, W. Nicolazzi, A. Bousseksou, *Adv. Mater*. **2018**, *30*, 17003862(1-23); (b) K. S. Kumar, M. Ruben, *Coord. Chem. Rev*. **2017**, *346*, 176-205; (c) J. Dugay, M. Arts, M. Giménez-Marqués, T. Kozlova, H. W. Zandbergen, E. Coronado, H. S. J. van der Zant, *NanoLett*. **2017**, *17*, 186-193.

[3] P. Gütlich, H.A. Goodwin, *Top. Curr. Chem*. **2004**, *233*, 1–47

[4] M. A. Halcrow, (Ed.) John Wiley & Sons: Chichester, UK, 2013

[5] P. Gütlich, A. B. Gaspar, Y. Garcia Beilstein *J. Org. Chem*. **2013**, *9*, 342–391.

[6] G. Aromí, L. A. Barrios, O. Roubeau, P. Gamez, *Coord. Chem. Rev*. **2011**, *255*, 485–546.

[7] O. Roubeau, *Chem. Eur. J*. **2012**, *18*, 15230-15244.

[8] L. G. Lavrenova, O. G. Shakirova, *Eur. J. Inorg. Chem*. **2013**, 670-682.

[9] O. Kahn, C. Jay Martinez, *Science* **1998**, *279*, 4479-4492

[10] J.-F. Létard, P. Guionneau, L. Goux-Capes, *Top. Curr. Chem*. **2004**, *235*, 221-249.

[11] L. Salmon, L. Catala, *C.R. Chimie* **2018**, *21*, 1230.

[12] (a) E. Coronado, J. R. Galán-Mascarós, M. Monrabal-Capilla, J. García-Martínez, P. Pardo-Ibáñez, *Adv. Mater*. **2007**, *19*, 1359-1361; (b) C. Bartual-Murgui, E. Natividad, O. Roubeau, *J. Mater. Chem. C.*, **2015**, *3*, 7916-7924.

[13] (a) I. A. Gural'skiy, C.M. Quintero, G. Molnar, I. O. Fritsky, L. Salmon, A. Bousseksou, *Chem. Eur. J*. **2012**, *18*, 9946-9954; (b) S. Rat, M. Piedrahita-Bello, L. Salmon, G. Molnár, P. Demont, and A. Bousseksou, *Adv. Mater*. **2018,** *30*, 1705275; (c) I. Imaz, D. Maspoch, C. Rodríguez-Blanco, J.M. Pérez-Falcón, J. Campo, and D. Ruiz-Molina, *Angew. Chemie - Int. Ed. Engl*. **2008**, *47*, 1857-1860.

[14] N. Daro, L. Moulet, N. Penin, N. Paradis, J.-F. Létard, E. Lebraud, S. Buffière, G. Chastanet, P. Guionneau, *Materials*, **2017**, *10*, 60(1-13).

[15] J.H. González-Estefan, M. Gonidec, N. Daro, M. Marchivie, and G. Chastanet, *Chem. Commun*. **2018**, *54*, 8040-8043.

[16] S. Marre, K.F. Jensen, *Chem. Soc. Rev*. **2010**, *39*, 1183-1202.

[17] R. M. Myers, D. E. Fitzpatrick, R. M. Turner, S. V. Ley, *Chem. Eur. J.* **2014**, *20*, 12348-12366.

[18] J. Pan, A. O. El-Ballouli, L. Rollny, O. Voznyy, V. M. Burkalov, A. Goriely, E. H. Sargent, O. M. Bakr, *ACS Nano* **2013**, *7*, 10158-10166.

[19] Chakrabarty, S. Marre, R.F. Landis, V. Rotello, U. Maitra, A. Del Guerzo, C. Aymonier, *J. Mater. Chem. C* **2015**, *3*, 7561-7566.

[20] Giroire, S. Marre, A. Garcia, T. Cardinal, C. Aymonier, *React. Chem. Eng*. **2016**, *1*, 151-155.

[21] S. Marre, J. Park, J. Rempel, J. Guan, M. G. Bawendi, K. F. Jensen, *Adv. Mater*. **2008**, *20*, 4830-4834.

[22] P. Laurino, R. Kikkeri, P. H. Seeberger, *Nat. Protocols* **2011**, *6*, 1209-1220.

[23] S. E. Lohse, J. R. Eller, S. T. Sivapalan, M. R. Plews, C. J. Murphy, *ACS Nano* **2013, *7***, 4135-4150.

[24] K. J. Hartlieb, M. Saunders, R. J. J. Jachuck, C. L. Raston, *Green Chem* **2010**, *12*, 1012-1017.

[25] N. Chan, M. F. Cunningham, R. A. Hutchinson, *Polym. Chem*. **2012**, *3*, 1322-1333.

[26] C. H. Hornung, C. Guerrero-Sanchez, M. Brasholz, S. Saubern, J. Chiefari, G. Moad, E. Rizzardo, S. H. Thang, *Org. Process. Res. Dev.* **2011**, *15*, 593-601.

[27] M. Gimeno-Fabra, A. S. Munn, L. A. Stevens, T. C. Drage, D. M. Grant, R. J. Kashtiban, J. Sloan, E. Lester, R. I. Walton, *Chem. Commun*. **2012**, *48*, 10642-10644.

[28] L. D'Arras, C. Sassoye, L. Rozes, C. Sanchez, J. Marrot, S. Marre, C. Aymonier, *New. J. Chem*. **2014**, *38*, 1477-1483.

[29] Pagnoux-Ozherelyeva, D. Bolien, S. Gaillard, F. Peudru, J.-F. Lohier, R. J. Whitby, J.-L. Renaud, *J. Organomet. Chem*. **2014**, *774*, 35-42.

[30] H. Seyler, S. Haid, T.-H. Kwon, D. J. Jones, P. Bäuerle, A. B. Holmes, W. W. H. Wong, *Aust. J. Chem*. **2013**, *66*, 192-198.

[31] Y. Nakano, G. P. Savage, S. Saubern, P. J. Scammells, A. Polyzos, *Austr. J. Chem*. **2013**, *66*, 178-182.

[32] Z. Yu, X. Xie, H. Dong, J. Liu, W. Su, *Org. Process Res. Dev.* **2016**, ***20***, 774-779.

[33] J. Ma, S. M. Lee, C. Yi, C.-W. Li, *Lab Chip*, **2017**, *17*, 209-226

[34] F. Zhang, S. Marre, A. Erriguible, *Chemical Engineering Journal,* **2020**, *382*, 122859-122871.

[35] T. Jahouri, F. Zhang, T. Tassaing, S. Fery-Forgues, C. Aymonier, S. Marre, A. Erriguible, *Chemical Engineering Journal,* **2020,** Accepted for publication

[36] K. Robertson, P.-B. Flandrin, H. J. Shepherd, C. C. Wilson, *Chimica Oggi – Chemistry Today*, **2017**, *35*(1), 2-5.

[37] J. Kröber, J.-P. Audière, R. Claude, E. Codjovi, O. Kahn, J.G. Haasnoot, F. Grolière, C. Jay , A. Bousseksou, J. Linarès, F. Varret, A. Gonthier-Vassal, *Chem. Mater*. **1994**, *6*, 1404-1412.

[38] J.G. Haasnoot, G. Vos, W.L. Groeneveld, *Z. Naturforsch*. **1977**, *32b*, 1421-1430.

[39] J.-F. Létard, N. Daro, O. Nguyen, Patent WO2007/065996; (b) T. Forestier, S. Mornet, N. Daro, T. Nishihara, S. I. Mouri, K. Tanaka, O. Fouché, E. Freysz, J.-F. Létard, *Chem. Commun*. **2008**, 4327-4329; (c) D. Mader, S. Pillet, C. Cateret, M. J. Stébé, J. L. Blin, *J. Dispers. Sci. Sci. Technol*. **2011**, *32*, 1771-1779; (e) T. Forestier, A. Kaiba, S. Pechev, D. Denux, P. Guionneau, C. Etrillard, N. Daro, E. Freysz, J.-F. Létard, *Chem. Eur. J*. **2009**, *15*, 6122-6130; (f) J.R. Galán-Mascarós, E. Coronado, A. Forment-Aliaga, M. Monrabal-Capilla, E. Pinilla-Cienfuegos, M. Ceolin, *Inorg. Chem*. **2010**, *49*, 5706-5714; (g) A. Tokarev, L. Salmon, Y. Guari, G. Molnár, A. Bousseksou, *New. J. Chem*. **2011**, *35*, 2081-2088.

[40] Grosjean, P. Négrier, P. Bordet, C. Etrillard, D. Mondieig, S. Pechev, E. Lebraud, J.-F. Létard, P. Guionneau, *Eur. J. Inorg. Chem*. **2013**, 796–802.

[41] P. Durand, S. Pillet, E. Bendeif, C. Carteret, M. Bouazaoui, H. El Hamzaoui, B. Capoen, L. Salmon, S. Hébert, J. Ghanbaja, L. Aranda, D. Schaniel, *J. Mater. Chem. C* **2013**, *1*, 1933–1942.

[42] L. Moulet, N. Daro, C. Etrillard, J.-F. Létard, A. Grosjean, P. Guionneau, *Magnetochemistry* **2016**, *2*, 10.

[43] R. L. Hartman, J. P. McMullen, K. F. Jensen, *Angew. Chem. Int. Ed*. **2011**, *50*, 7502-7519.

Entry for the Table of Contents

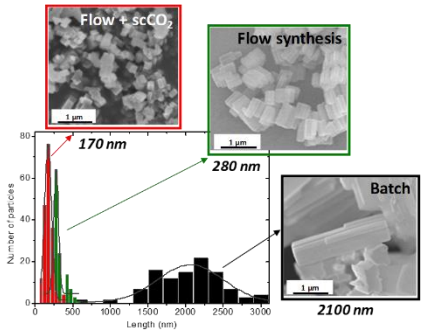

We report here an innovative and robust template-free continuous process to synthesize nanoparticles of a switchable coordination polymer, including the use of supercritical CO_2, aiming at both quenching the particle growth and drying the powder.